Supporting information

Low-hysteresis and highly linear sensors based on environmentally stable, adhesive, and antibacterial hydrogels

Chengmeng Wei,[a] Yao Wang,[a] Yongjie Liang,[a] Jiaming Wu,[a] Feng Li,[a] Qiuxia Luo,[a] Yewei Lu,[a] Cuiwen Liu,[a] Ru Zhang,[a] Zhenpin Lu,[b] Baiping Xu,[a] Ning Qing,[a,]* Liuyan Tang[a,]*

[a] School of Environmental and Chemical Engineering, Wuyi University, Jiangmen, 529020, China.

[b] Department of Chemistry, City University of Hong Kong, Hong Kong, 999077, China.

*Corresponding author.

E-mails: tangly@wyu.edu.cn(wyuchemtangly@126.com) (Liuyan Tang), wyuchemqn@126.com (Ning Qing)

Table S1. The detailed formulation of PVA-PA-E/M hydrogels

EA (mol/L)	MPTC (mol/L)	EA/MPTC
0.075	**1.10**	**0.1**
0.15	**1.05**	**0.14**
0.2	**1.04**	**0.2**
0.3	**1.01**	**0.3**
0.4	**0.98**	**0.4**
0.5	**0.95**	**0.5**

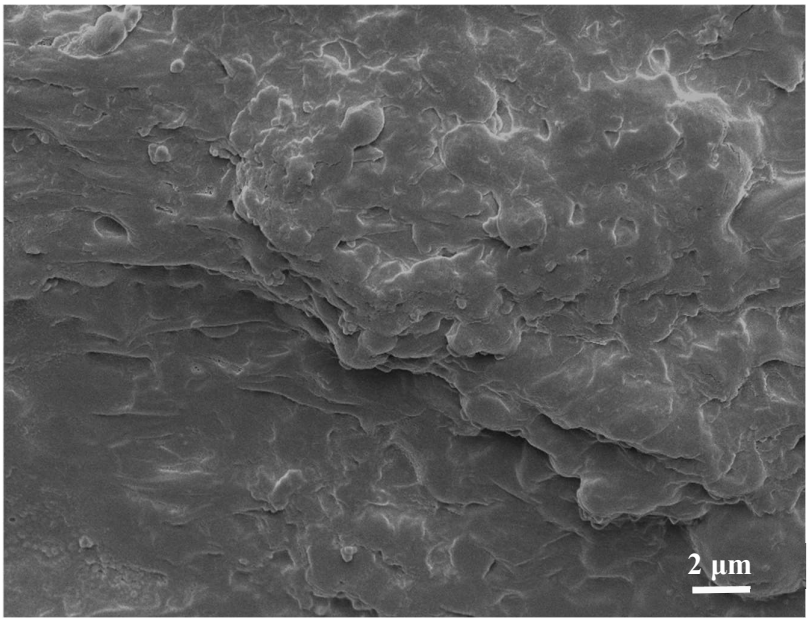

Fig. S1. SEM image of PVA-E/$M_{0.4}$ hydrogel.

Elements proportion

Element	C-Atomic%	N-Atomic%	O-Atomic%	P-Atomic%	Cl-Atomic%
Atomic	50.42	5.20	34.96	8.11	1.32

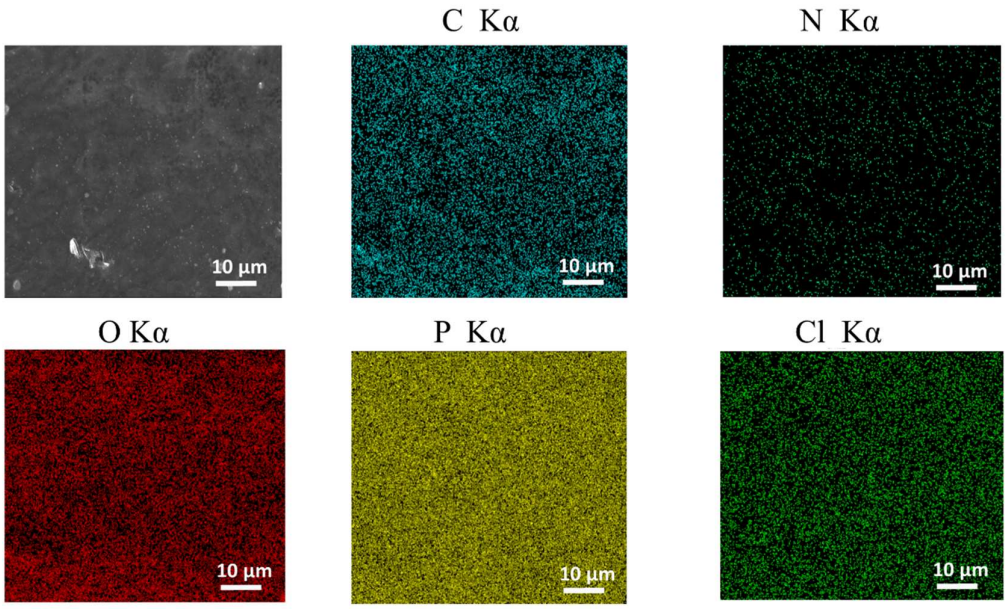

Fig. S2. EDS proportion and element images of PVA-E/$M_{0.4}$ hydrogel.

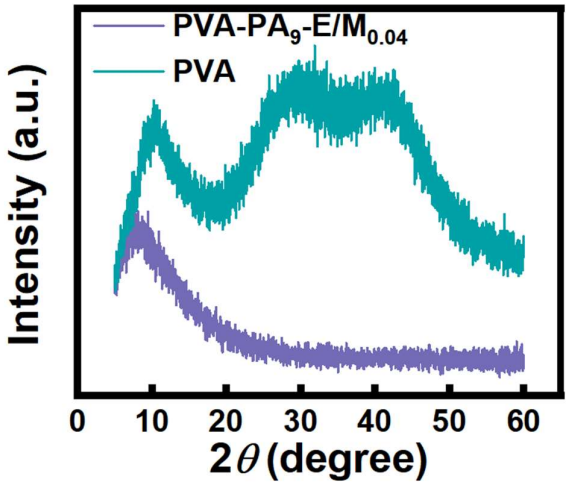

Fig. S3. XRD spectra of the PVA and PVA-PA_9-$E/M_{0.4}$ hydrogel.

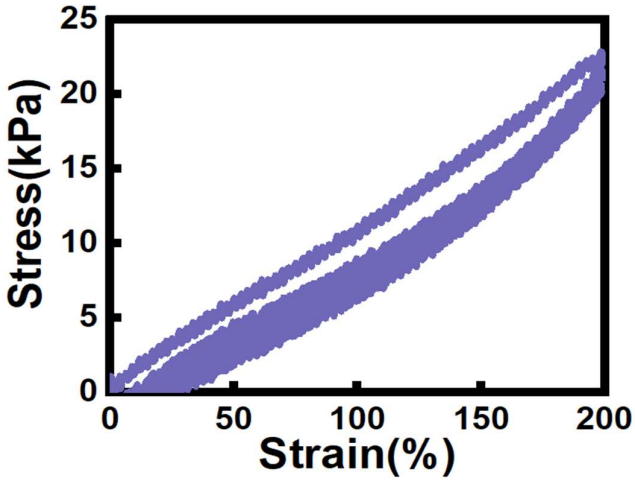

Fig. S4. 10 continuous loading-unloading cycles of PVA-PA_9-E/$M_{0.4}$ hydrogel at a strain of 200%.

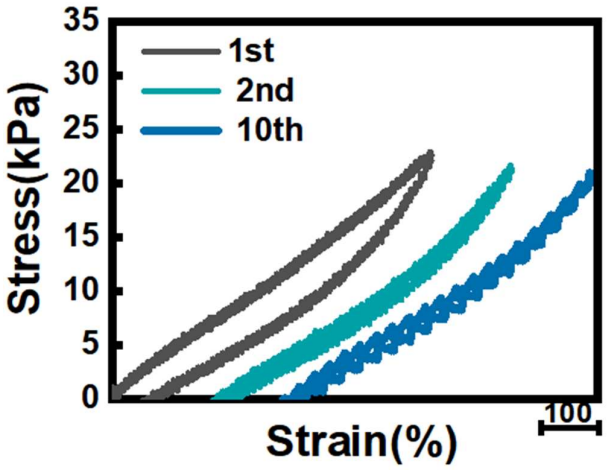

Fig. S5. The 1st, 2nd, and 10th loading-unloading cycles of PVA-PA_9-E/$M_{0.4}$ hydrogel at a strain of 200%.

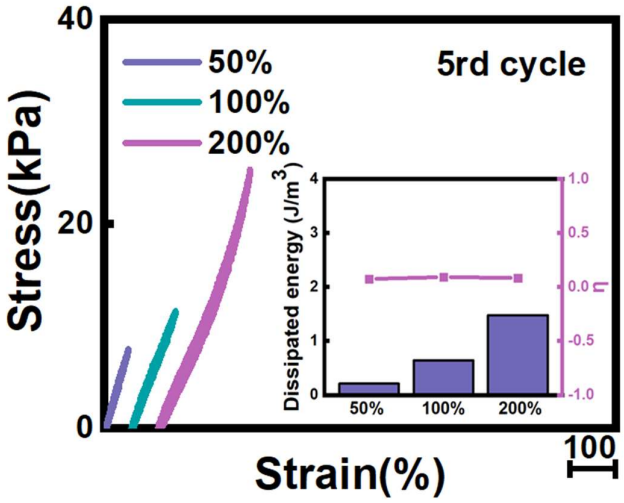

Fig. S6. Loading-unloading cycles of PVA-PA$_9$-E/M$_{0.4}$ hydrogel at different applied strains. The insets correspond to the dissipated energy and mechanical hysteresis of these cycles.

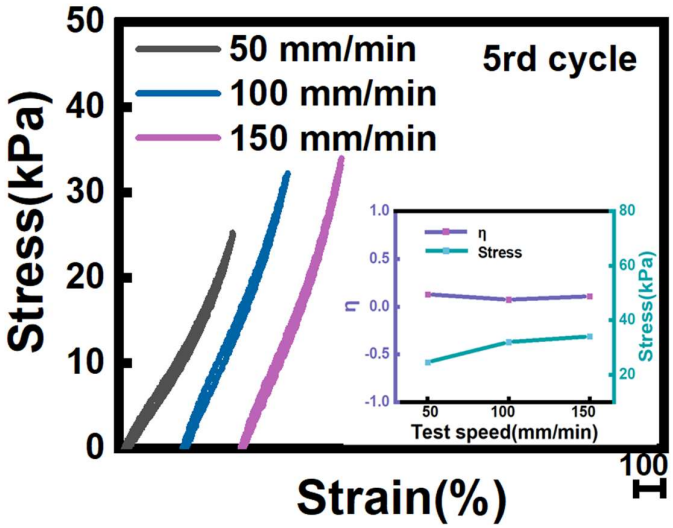

Fig. S7. Loading-unloading cycles of PVA-PA_9-E/$M_{0.4}$ hydrogel at different strain speeds. The insets correspond to the fracture stress and mechanical hysteresis of these cycles.

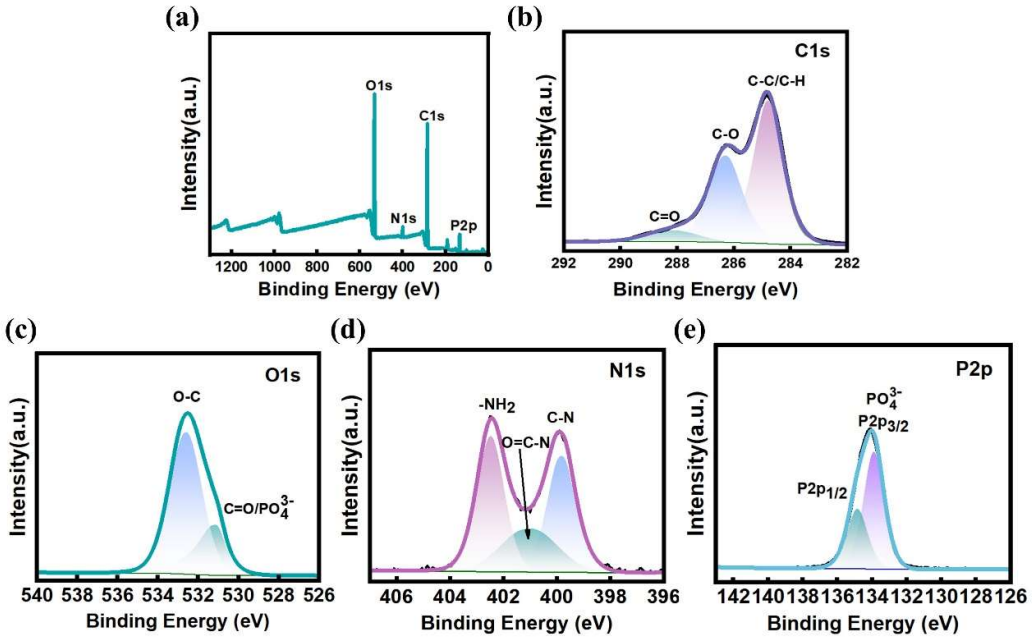

Fig. S8. The XPS spectra of PVA-PA_9-E/$M_{0.4}$ hydrogel kept at room temperature. (a) XPS survey spectra. (b) C 1s scan. (c) O 1s scan. (d) N 1s scan. (e) P 2p scan.

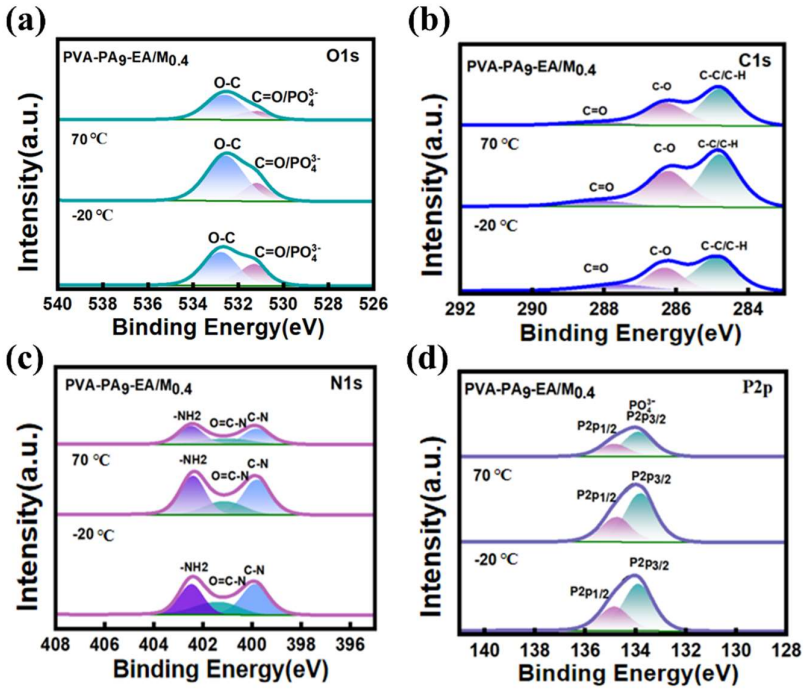

Fig. S9. The XPS spectra of PVA-PA_9-E/$M_{0.4}$ hydrogel treated at different temperatures. (a) O 1s scan. (c) C 1s scan. (d) N 1s scan. (e) P 2p scan.

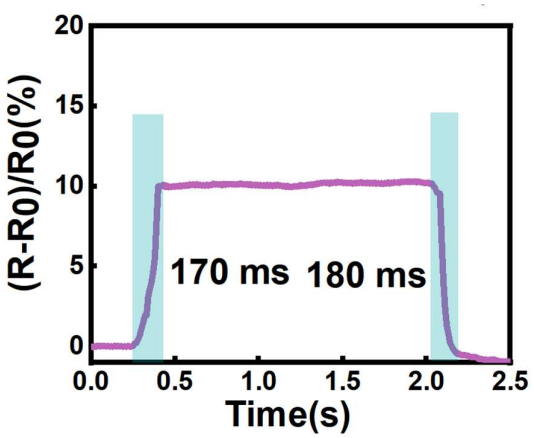

Fig. S10. Response and recovery time of the hydrogel sensor under 15% strain.

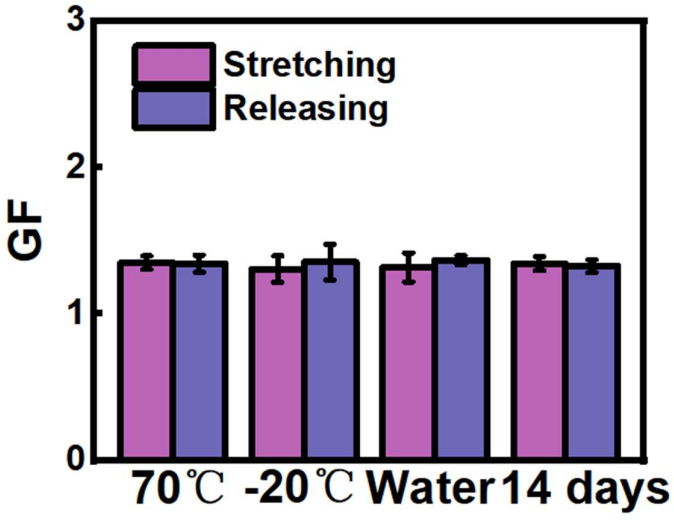

Fig. S11. GF of PVA-PA_9-E/$M_{0.4}$ hydrogel-based strain sensor under different environments.

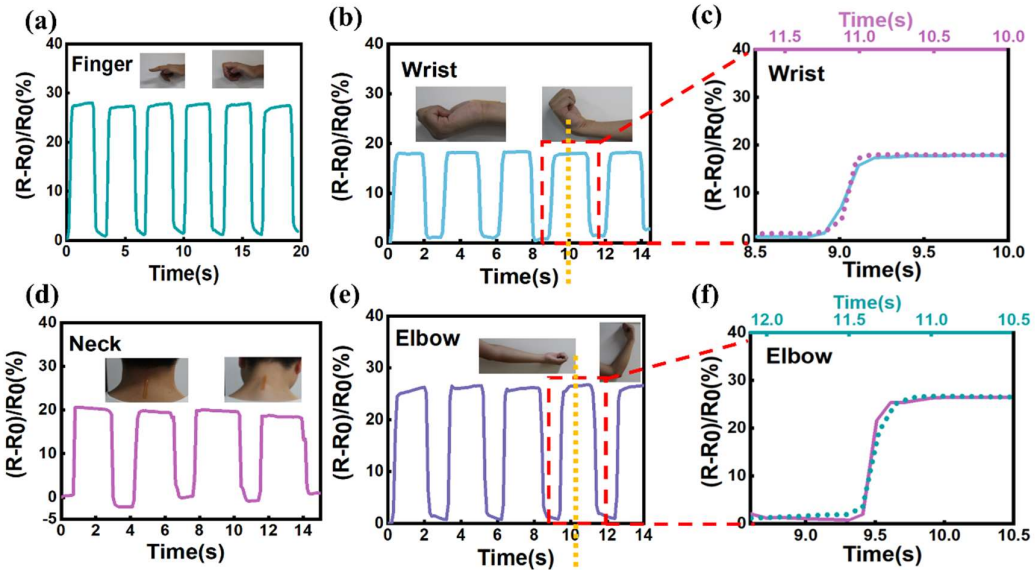

Fig. S12. The relative resistance changes of PVA-PA_9-E/$M_{0.4}$ hydrogel-based strain sensor in response to (a) finger, (b) wrist, (d) neck, and (e) elbow bending. The figures displaying the symmetry of the bending and releasing signals in the same cycle of (c) wrist and (f) elbow bending.

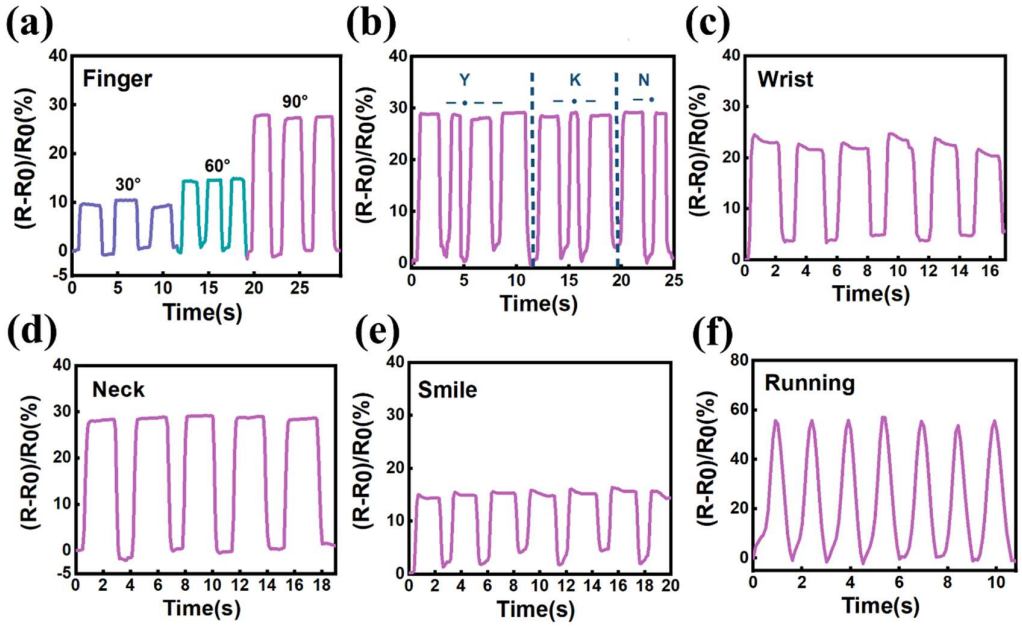

Fig. S13. The relative resistance changes of PVA-PA_9-E/$M_{0.4}$ hydrogel-based strain sensor in response to various human motions at 70 °C.

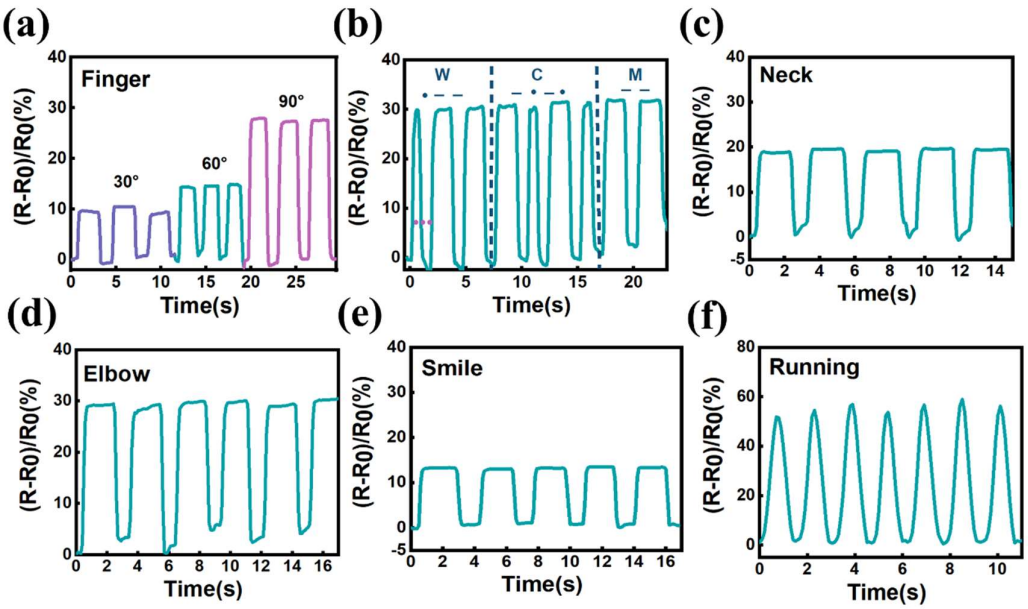

Fig. S14. The relative resistance changes of PVA-PA_9-E/$M_{0.4}$ hydrogel-based strain sensor in response to various human motions at -20 °C.

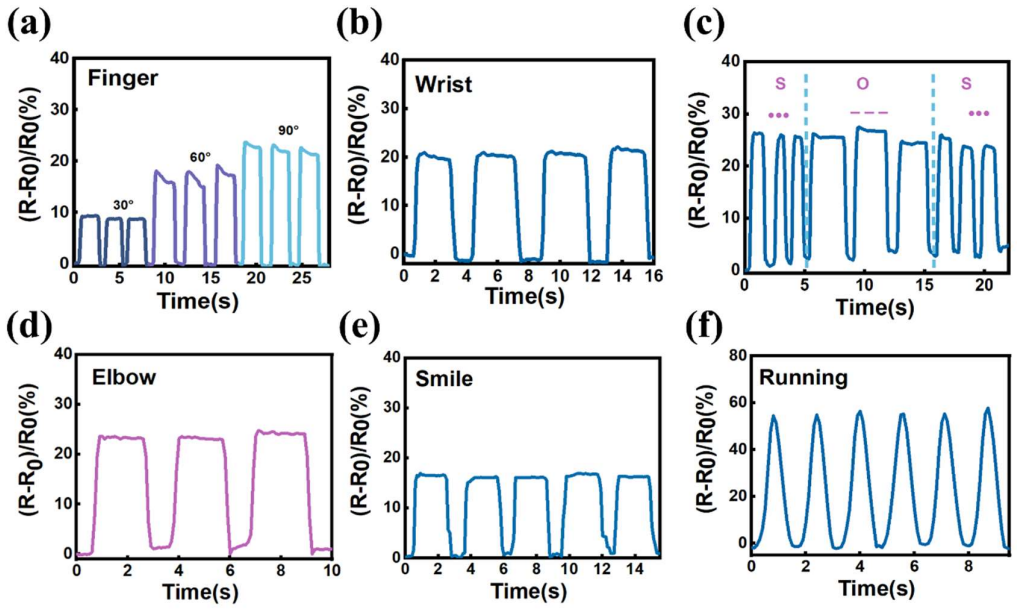

Fig. S15. The relative resistance changes of PVA-PA_9-E/$M_{0.4}$ hydrogel-based strain sensor in response to various human motions after water immersion.

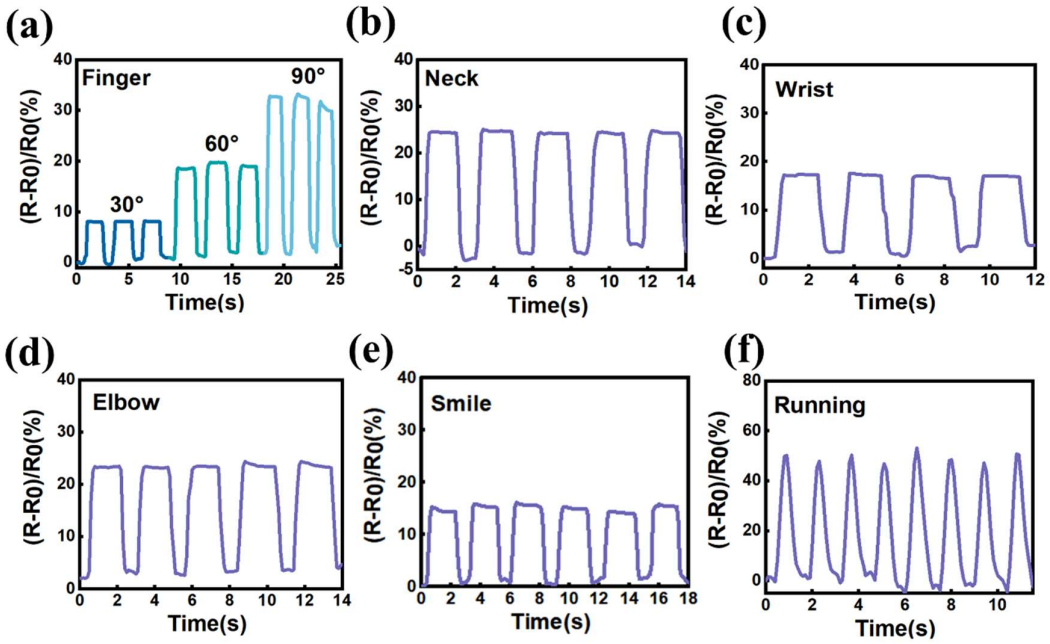

Fig. S16. The relative resistance changes of PVA-PA_9-E/$M_{0.4}$ hydrogel-based strain sensor in response to various human motions after 14-day storage.

Table S2. Comparison of the strain sensor in this work with other reported hydrogel-based strain sensors.

Hydrogel	Low hysteresis	Adhesion property (kPa)	Linearity	GF	Environmental stability	Conductivity ($S\ m^{-1}$)	Ref
SFRHs	No	No	No	0.82-2.67	Yes (under water)	3.93	1
PVA-CNF	No	No	No	0.96-1.57	Yes (50 °C, -50°C, long-term storage)	NA	2
CNC/CMC-Na/PVA	No	No	No	1.00-1.40	Yes (-70 °C)	2.1	3
SF/TA@PPy	No	~38	No	0.72	Yes (under water)	0.034	4
ionogel-NTf_2	No	~35	No	0.40-0.69	No	3.5×10^{-3}	5
PPHM	No	32.7	No	2.05-4.82	Yes (-20 °C)	0.06	4
FG-Ag	No	14	No	3.11-4.00	No	N.A.	6
CareGum	No	144	No	0.50-1.04	No	1.0	7
PVA–CS–PA hydrogels	No	No	Yes (0~900%, R^2=0.996)	1.31-2.60	Yes (long-term storage)	0.48	8
PVA/CNCs @PDA-AuNPs	No	No	Yes (0~350%, R^2=0.998)	0.99	No	~0.30	9
PAM-TSAS N_2-$LiCl_5$	Yes (~0.1)	12	No	1.45-4.50	No	0.4	10
LSN-1.5-Fe/ PAM	Yes (0.15)	11.6	Yes (0~100%, R^2=0.996)	1.22	No	0.16	11
PVA-PA_9-E/ $M_{0.04}$	Yes (0.0356)	70.95	Yes (0~300%, R^2=0.999)	1.34	Yes (70 °C, -20°C, long-term storage, and water environments)	6.55	This work

*NA = not available

Reference

1 X. Lu, Y. Si, S. Zhang, J. Yu and B. Ding, *Adv. Funct. Mater.*, 2021, **31**, 1–9.

2 X. Chu, R. Wang, H. Zhao, M. Kuang, J. Yan, B. Wang, H. Ma, M. Cui and X. Zhang, *ACS Appl. Mater. Interfaces*, 2022, **14**, 16631–16640.

3 H. Wang, Z. Li, M. Zuo, X. Zeng, X. Tang, Y. Sun and L. Lin, *Carbohydr. Polym.*, 2022, **280**, 119018.

4 H. Zheng, M. Chen, Y. Sun and B. Zuo, *Chem. Eng. J.*, 2022, **446**, 136931.

5 Y. Zhao, D. Gan, L. Wang, S. Wang, W. Wang, Q. Wang, J. Shao and X. Dong, *Adv. Mater. Technol.*, 2023, **8**, 1–10.

6 R. Yan, Q. Sun, X. Shi, Z. Sun, S. Tan, B. Tang, W. Chen, F. Liang, H. D. Yu and W. Huang, *Nano Energy*, 2023, **118**, 108932.

7 F. B. Kadumudi, M. Hasany, M. K. Pierchala, M. Jahanshahi, N. Taebnia, M. Mehrali, C. F. Mitu, M. A. Shahbazi, T. G. Zsurzsan, A. Knott, T. L. Andresen and A. Dolatshahi-Pirouz, *Adv. Mater.*, 2021, **33**, 1–14.

8 C. Liu, R. Zhang, Y. Wang, J. Qu, J. Huang, M. Mo, N. Qing and L. Tang, *J. Mater. Chem. A*, 2023, **11**, 2002–2013.

9 P. Li, Z. Ling, X. Liu, L. Bai, W. Wang, H. Chen, H. Yang, L. Yang and D. Wei, *Chem. Eng. J.*, 2023, **466**, 143306.

10 S. Han, H. Tan, J. Wei, H. Yuan, S. Li, P. Yang, H. Mi, C. Liu and C. Shen, *Adv. Sci.*, 2023, **10**, 1–12.

11 H. Zhao, S. Hao, Q. Fu, X. Zhang, L. Meng, F. Xu and J. Yang, *Chem. Mater.*, 2022, **34**, 5258–5272.